Optimizing Point Cloud Processing for Facial Reconstruction Using Open-Source Tools: A Preliminary Study

Ena Barčić, Petra Grd
University of Zagreb
Faculty of Organization and Informatics
Pavlinska 2, Varaždin, Croatia
{enbarcic, petra.grd}@foi.unizg.hr

Abstract. *In this preliminary study, we present the first step in point cloud processing for the creation of bone and skin models for facial reconstruction, while focusing on what can be achieved using open-source tools. Through our experiment, we achieved an average reduction of 91.13% in point cloud models size for the skull and 80.35% for the skin model. The results demonstrate the feasibility of optimizing point cloud data, enabling more efficient storage, processing, and analysis for facial reconstruction. This study lays the foundation for further research in point cloud processing to enhance the efficiency and accuracy of facial models.*

Keywords. digital facial reconstruction, point clouds, data size, open-source tools

1 Introduction

Digital facial reconstruction (DFR), the process of recreating the facial features of an individual based on skeletal remains (Miranda et al., 2018), plays a critical role in forensic anthropology and the identification of unknown individuals. With the advance of digital technologies, there has been a shift towards the utilization of 3D modeling and visualization techniques. Point cloud models, even though a very new approach, have become increasingly prevalent in these applications due to their ability to accurately represent the surface geometry of facial structures. However, the growing complexity and size of point cloud data poses a challenge in terms of storage, processing, and computational efficiency. By reducing the size of point clouds, while preserving essential anatomical details, the presented method aims to optimize computational resources and streamline the facial reconstruction workflow.

Point clouds have distinct advantages over mesh techniques in forensic facial reconstruction, particularly when an accurate representation of both skeletal and facial anatomy is essential. Point clouds, being sets of three-dimensional points that capture the shape and position of facial features, allow for a more precise depiction of facial morphology and skeletal landmarks. Unlike meshes, which rely on surface interpolation and can sometimes oversimplify complex anatomical structures.

DFR offers numerous advantages over traditional methods, including speed, automation, and standardization (Miranda et al., 2018). Today, head CT (computed tomography) scans are most commonly utilized as a base for creating new DFR models. From CT images, point clouds can be created using Digital Imaging and Communications in Medicine (DICOM) data, representing a dense collection of individual measurement points with x, y, and z coordinates (Ulinuha et al., 2019). The flexibility of point cloud-based models allows for the precise placement of points within the 3D space, enabling extremely accurate localization of facial landmarks and features. This approach not only provides a more realistic visualization but also allows for quantitative measurements and comparisons.

Open-source tools have emerged as valuable resources in various scientific domains, and DFR is no exception. These tools offer researchers and forensic professionals access to freely available software libraries, algorithms, and frameworks that can be customized and extended for specific applications (Simmons-Ehrhardt et al., 2018). Leveraging open-source tools in this preliminary study enables the exploration of their potential in generating and analyzing point cloud data for DFR.

In the following sections, we will discuss the methodology employed for generating point cloud-based models from CT scans, the techniques used for point cloud creation, the analysis and evaluation of the created point clouds, the open-source tools, and the implications and limitations of this preliminary study.

2 Related work

DFR has been a topic of significant interest and research within the fields of forensic anthropology, computer vision, and medical imaging. This section provides an overview of related works and advancements in the field, highlighting key contributions and method-

ologies employed in the pursuit of more effective and precise DFR.

One of the first papers on DFR was (da Costa Moraes et al., 2014), where the authors present a protocol for computer-aided DFR using free software and photogrammetry. While they initially used a point cloud model, they converted it into a mesh using MeshLab. They focused on anatomical modeling of the facial features which resulted in the process being rather long and relying on virtual soft tissue pegs that were placed by hand for their final reconstruction. Similarly, the authors in (Simmons-Ehrhardt et al., 2018) present their approach to dense facial tissue depth mapping (DFTDM) of CT models using open-source tools. The authors generated DFTDM on hollowed, cropped face shells using the Hausdorff sampling. They used point clouds to perform the tissue depth measurements and found that minimum depth values ranged from 1.2 mm to 3.4 mm. Maximum depths were found in the buccal region and neck, excluding the nose.

Some of the earliest and most notable examples of CT scan usage can be seen in (Ulinuha et al., 2019) where the authors focus on creating a protocol for the extraction of skull and face surfaces from CT images. They focus on the problem of CT image size and were among the first authors to identify point clouds as a potential solution. Their extraction process produces point clouds with an average file size of 9.1% of the size of the original CT image file. In (Hargreaves et al., 2021) the authors present a generative deep learning approach for DFR directly from the bone with limited data and no background expertise. Their model is trained on 665 CT head scans that have been cleaned of noise, rotated to the correct orientation, and then filtered by density to find the bone and soft tissue to be used as the input and label respectively. They were able to achieve a facial detection score of 88.32%. Lastly, the authors (Duan et al., 2015) focus on 3D face reconstruction from the skull by regression modeling in shape parameter spaces. DFR is realized by using the relationship between the real face and the face statistical shape model. The skull and face are divided into five corresponding feature regions, and a mapping from each skull region to the corresponding face region is established. Their dataset consisted of 114 whole-head CT scans from the Han ethnic group in the North of China. They use dense meshes to represent the face and skull.

A popular approach is the creation of DFR models based on specific populations and STT. These are also the papers that put the largest emphasis on creating large-scale and population-specific databases. In (Ma et al., 2011), the authors focus on building a Vietnam-specific DFR based on STT and geometric proportions. Their database consists of full-head CT scans of 959 individuals. However, they still rely on manual landmarks and STT marker placement. They present one of the first approaches with deformable landmark-based templates and the addition of their own landmarks. The authors are able to achieve errors between 1.17mm to 1.24mm in two cases, which are some of the lowest errors achieved at the time. Additionally, the authors (Shui et al., 2010) present a China-specific DFR and build their own database, which consists of more than 200 full-head CT scans of Chinese people from both north and south China. They use thin-plate spline (TPS) to achieve non-rigid registration between the unidentified skull and reference skull and then choose a reference template. They also use a region-based approach reconstructing the face, nose, and mouth separately. In the end, the authors were able to achieve high-accuracy results in the coronal and mandible regions.

3 Creation of point cloud models

In this section, we present the main challenges to DFR, together with the tools and the dataset used in this study.

3.1 Challenges

While looking at the previously described research papers, we were able to identify several key challenges in the field of DFR:

One of the biggest challenges is the low availability of CT datasets. Obtaining a diverse and representative dataset that includes individuals from different populations and age groups is crucial to ensure the accuracy and generalizability of the reconstructed faces. In addition, the available datasets are all very small in size. To address this challenge, efforts should be made to expand the existing datasets by collaborating with forensic institutions, medical facilities, and research organizations to collect and share relevant CT scans and associated metadata. Finally, there are no "clean" publicly available datasets for DFR. Most of the available datasets fall into three categories: brain CT scans that tend not to contain the lower jaw, head and neck scans that tend not to contain the top part of the skull and mixed sets.

In addition, point clouds are not well-studied in the field of DFR. While point cloud data has gained recognition in various fields, including computer vision and 3D modeling, its application in DFR is relatively unexplored. The lack of in-depth studies and established methodologies for handling point cloud data specifically for DFR presents a challenge in optimizing the use of this data format.

Another challenge we identified was the limited capacity of open-source tools for point cloud processing. Open-source tools, such as MeshLab, have been widely used in the field of 3D modeling and reconstruction. However, when it comes to point cloud processing, these tend to have limited capabilities when compared to mesh models. Point cloud data requires specialized

algorithms for processing, registration, and manipulation, which tend to not be fully supported by existing open-source tools.

Furthermore, a relatively small number of research publications focused specifically on point cloud-based facial reconstructions. The field is still evolving, and while there is a growing interest in utilizing point cloud data, the number of published studies addressing its challenges and advancements remains relatively small.

A prominent problem is also the lack of standardized protocols and guidelines in the field of DFR, specifically for point cloud protocols. The absence of widely accepted standardized protocols and guidelines in DFR can lead to inconsistencies and discrepancies in the reconstruction process. Establishing a unified set of guidelines, including data acquisition, landmark placement, and facial approximation techniques, is essential to enhance the reliability and replicability of DFR across different forensic cases.

Addressing these challenges will require collaborative efforts from researchers, forensic practitioners, and software developers. Overcoming these obstacles will not only enhance the accuracy and efficiency of DFR, but also contribute to the development of standardized methodologies and tools that can be adopted by the forensic community at large.

3.2 Computed tomography (CT)

CT images have proven to be invaluable in the field of DFR, providing a wealth of anatomical information for accurate facial analysis. They allow detailed visualization of the craniofacial region, including the bones, soft tissues, and underlying structures. This imaging method captures high-resolution cross-sectional images, enabling forensic investigators to examine the intricate details of the skull and facial features. By leveraging advanced software tools, present in open-source programs, such as segmentation algorithms and 3D visualization, forensic professionals can manipulate the CT image data to extract the facial structures and generate accurate digital models for further analysis. The use of CT images in DFR enhances the ability to recreate the individual's appearance and supports investigative efforts in identifying the deceased or missing persons, contributing to the resolution of criminal cases and providing closure to families and communities.

3.3 Tools

The tools used in this research were chosen based on analyzed research in the field of DFR. The tools had to be free to use and verified in at least one other research paper.

3D Slicer (3D Slicer image computing platform, 2023) is a widely utilized open-source tool in the field of medical imaging and DFR, particularly used for CT images. With its user-friendly interface and powerful capabilities, 3D Slicer enables efficient segmentation, visualization, and manipulation of CT images, facilitating the extraction of meaningful information from complex datasets. By leveraging advanced algorithms and interactive visualization tools offered by 3D Slicer, forensic investigators can accurately assess facial features, perform bone/skin segmentation, and much more. This enables aiding in the identification and comparison components for individuals in forensic investigations.

MeshLab (Cignoni et al., 2008) is a powerful open-source tool that has found significant applications in DFR. It is also one of the few open-source tools that support the analysis of point cloud data. With its comprehensive set of tools and features, MeshLab provides a valuable platform for processing, editing, and analyzing 3D geometric models, including point clouds obtained from various sources, such as laser scanners or CT segmentations. By utilizing its advanced algorithms, users can refine and manipulate the models, enhancing the level of detail and accuracy necessary for facial analysis. Moreover, MeshLab facilitates measurements and comparisons of facial landmarks, aiding in the identification of individuals or the assessment of facial asymmetry and morphological variations.

CloudCompare (CloudCompare - Open Source project, 2023) is an open-source tool that plays a crucial role in the comparison of facial and bone point clouds. CloudCompare enables researchers and practitioners to perform detailed analysis and alignment of 3D point cloud data. In the context of facial and bone point clouds, this tool proves invaluable for assessing and quantifying the degree of correspondence between these two sets of data. By utilizing various algorithms and techniques provided by CloudCompare, such as registration, surface comparison, and distance measurements, researchers can precisely evaluate the alignment accuracy and spatial relationships between facial and bone point clouds.

3.4 Dataset

The CQ500 head CT dataset (CQ500 - V7 Open Datasets, 2023), provided by the Centre for Advanced Research in Imaging, Neurosciences and Genomics (CARING) in New Delhi, India, serves as a valuable clinical validation dataset. It contains 491 head CT scans and is one of the largest freely available datasets made for research purposes. The dataset consists of head CT scans obtained using various CT scanner models. The CT scanners used in these centers had a slice per rotation ranging from 16 to 128, offering a diverse range of image data. The dataset was obtained by extracting anonymized data from local Picture Archiving and Communication System (PACS) servers in compliance with internally defined Health Insurance Portability and Accountability Act (HIPAA) guidelines. One notable feature of the CQ500 dataset is the availability

of clinical radiology reports associated with the scans, providing valuable context and additional information. The dataset was collected in two batches, with Batch B1 encompassing all head CT scans taken at the specified centers over a 30-day period starting from November 20, 2017. Batch B2 was selected using a natural language processing (NLP) algorithm, which identified specific pathologies.

4 Materials and methods

In this section, we present our experiment.

4.1 CT scan processing and segmentation

In our study, we employed 3D Slicer version 5.2.1 for CT image processing. This choice was driven by the extensive features and capabilities offered by 3D Slicer, making it suitable for our research objectives. The CT images used in our analysis were in DICOM format and were obtained from the CQ500 dataset. As the dataset consisted of both brain scans and slice scans, we had to manually refine it and choose 15 of the most complete head scans for our analysis with ten of those being considered as larger (contained the orbital and nasal area) and five being considered smaller scans (containing only the supraorbital region).

To extract relevant structures (bone and face skin) from the CT images, we employed thresholding techniques using Hounsfield units (HU) in 3D Slicer. HU values represent the density of tissues and materials in CT scans (Ulinuha et al., 2019). To achieve the best results, we started by applying automatic thresholding supported within 3D Slicer first for bone, and then for soft tissue. For the best results to be achieved, we then adjusted the values to best suit each individual scan for their respective bone and soft tissue values. To ensure the quality and accuracy of our segmentations, we took additional steps to filter out any impurities or residual equipment artifacts. This involved employing various techniques such as noise reduction and manual removal of unwanted elements. These preprocessing steps were crucial for obtaining clean and precise segmentations, minimizing any potential interference or inaccuracies in subsequent analyses. Once the segmentations were completed, we saved the resulting structures as Standard Tessellation Language (STL) files. STL is a commonly used file format for 3D models, making it compatible with a wide range of software and facilitating further analysis and visualization of the segmented structures. The preliminary results are presented in Figure 1.

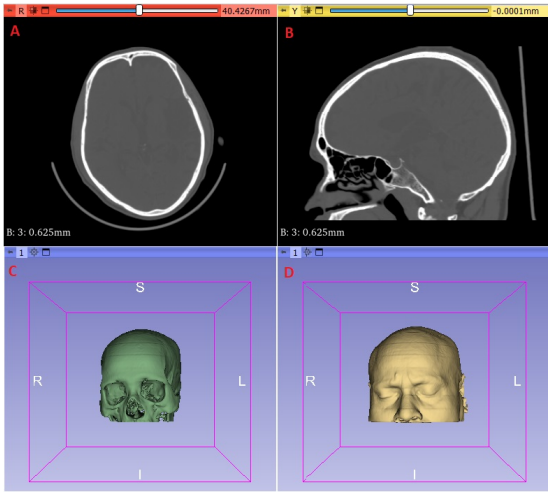

Figure 1: A and B original CT scan, C and D segmented 3D models

4.2 Point cloud creation and refinement

Next, we utilized MeshLab 2022.02 software for STL image processing, enabling comprehensive analysis and manipulation of the data. The STL images were loaded into MeshLab, providing a solid foundation for further processing steps. To ensure the accuracy and reliability of the data, we performed additional cleaning procedures, removing any artifacts or noise that may have been present in the original files. After the initial cleaning, the STL files were converted into point cloud format, enabling efficient handling and extraction of geometric information. The resulting data consisted of an average skull point cloud containing 980,939 points and an average face point cloud comprising 1,251,540 points. The preliminary point cloud models were saved as Polygon File Format or Stanford Triangle Format (PLY) files. The PLY format is a file format commonly used for storing 3D point cloud data. This representation provided a detailed and comprehensive depiction of the underlying geometry. An important advantage of point cloud data is the ability to precisely read and save the location of each point of the point cloud. This allows us to significantly reduce the number of points while still being able to reconstruct the original if it is needed.

To streamline the point cloud data, we removed all duplicate vertices. Duplicate vertices are multiple points that share the same coordinates. They can occur during data acquisition or processing, some of the most common reasons are errors in the data collection process, inaccuracies in scanning devices, or noise introduced during point cloud generation. They need to be removed to reduce data redundancy, improve processing speed and enhance the overall accuracy. To enhance the quality of the point cloud data, we applied a denoising process using the surface reconstruction screened poisson option in MeshLab. This algorithm utilized the oriented point sets to reconstruct watertight surfaces, effectively reducing noise and improving the overall accuracy of the point cloud data. The denoising step played a crucial role in refining the geometry and eliminating any unwanted artifacts or irregularities.

For further optimization, we employed point cloud simplification techniques, reducing the number of points while preserving the essential characteristics of the facial geometry. To confirm the model's accuracy we used the Compute Geometric Measures feature in Meshlab, making sure that the point clouds matched the original STL images using distance, area, and curvature measures. Through this process, we obtained an average simplified bone point cloud consisting of 72,039 points and an average simplified face point cloud comprising 199,747 points. This simplification step improved the computational efficiency and facilitated smoother data analysis. To ensure consistent alignment and comparison, we evaluated the normal vectors of the point sets. a normal vector represents the direction perpendicular to a surface at a specific point on that surface. When working with point clouds that represent surfaces (such as facial scans), normals can be evaluated at each point based on the surrounding points. Specifically, we compared the normals for each point with those of its neighboring points, with the number of neighbors set to 10. This step helped ensure accurate alignment and provided a reliable basis for subsequent measurements and comparisons.

4.3 Point cloud comparison and analysis

Finally, we utilized CloudCompare v2.13 for point cloud comparison. We wanted to determine whether the newly processed and original point clouds were properly aligned, if any distortions or outliers were present, and finally where the largest and smallest distances were measured, so that we can further focus on those areas in our continued research. We selected CloudCompare due to its renowned accuracy and reliability in measuring distances between point clouds. This choice ensured that our analysis was based on robust and dependable measurements. To begin the comparison process, we imported the point clouds (PLY files) into CloudCompare and aligned them accordingly. This alignment step was crucial to ensure proper spatial registration and enable accurate distance measurements. We also verified that the number of points in the point clouds was consistent and confirmed that it matched the numbers stated in the previous processing steps performed in MeshLab. This validation ensured consistency and provided confidence in the subsequent analysis.

Using the built-in compare distance functions in CloudCompare, we first calculated the distances between the newly processed point clouds and their original point cloud models and then conducted a comprehensive comparison of point cloud distances between the skull and skin point cloud models. This function allowed us to precisely measure the distances between corresponding points in the two point clouds, providing valuable insights into the variations and discrepancies between them. By leveraging the advanced capabilities of CloudCompare, we were able to conduct a detailed and accurate comparison of the point clouds, highlighting both the areas of agreement and areas of discrepancy. This information provided valuable insights into the spatial relationships and structural differences between the point clouds, enabling a comprehensive understanding of the variations in facial features and bone structures.

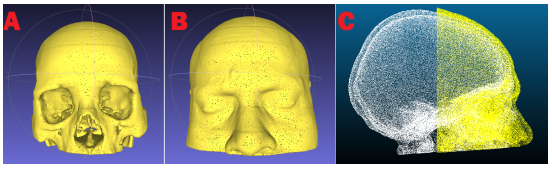

Figure 2: A and B preliminary dense point cloud models, C refined models

4.4 Point cloud acceptance criteria

In this study, we have set out 3 acceptance criteria. They were determined by criteria and best practices as seen in (Ulinuha et al., 2019, da Costa Moraes et al., 2014, Simmons-Ehrhardt et al., 2018, Hargreaves et al., 2021, Duan et al., 2015).

Visual appearance - the simplified point clouds had to undergo a visual inspection to assess their quality.

Noise and artifacts - noise, outliers, or artifacts in the simplified point cloud will be analyzed and needs to be nonexistent or kept at an acceptable minimal rate.

Alignment - newly created point clouds had to be aligned to the original mesh, preserving the shape of the originals.

5 Results

In our study, we aimed to present a preliminary point cloud reduction technique and analyze the variations in distance measurements when aligning, as well as compare the reduced point clouds. We were able to achieve a remarkable reduction in the sizes of the point clouds after processing. The results for the 15 analyzed CT scans are presented in Table 1.

Looking at the reduction percentages, we observe a consistent trend across all scans. For the skull, the reduction percentages range from 94.66% to 85.44%, while for the skin, they range from 87.69% to 68.10%. The findings demonstrate the effectiveness of the applied processing methods in achieving more streamlined and manageable point cloud models while preserving the essential anatomical details necessary for accurate DFR.

Examining the differences between the larger brain CT scans (scans 1-9 and 16) which contained both the orbital and nasal region and the smaller brain CT scans (scans 10-12 and 14, 15) which contained only the supraorbital region, we can observe that the reduction

Table 1: Results of point cloud reduction

Scan ID	Bone org.	Skin org.	Bone proc.	Skin proc.	Bone reduc.	Skin reduc.
1	1.159.590	2.045.188	61.924	281.910	94.65%	86.21%
2	1.120.242	2.028.364	77.528	277.887	93.07%	86.29%
3	1.102.358	1.445.892	76.585	213.907	93.05%	85.20%
4	1.192.294	1.417.956	80.645	205.808	93.23%	85.48%
5	1.339.260	1.481.048	87.839	199.328	93.44%	86.54%
6	1.360.758	1.459.832	79.263	186.797	94.17%	87.20%
7	1.361.004	1.530.458	79.196	194.076	94.18%	87.31%
8	1.322.850	1.409.420	70.568	200.176	94.66%	85.79%
9	1.328.444	1.644.510	72.701	202.355	94.52%	87.69%
10	454.076	484.502	65.712	152.372	85.52%	68.55%
11	444.036	474.766	64.411	150.623	85.49%	68.27%
12	478.280	489.290	68.142	153.354	85.75%	68.65%
13	1.156.004	1.888.552	66.217	267.902	94.27%	85.81%
14	443.306	479.806	64.502	153.039	85.44%	68.10%
15	451.582	493.520	65.347	156.673	85.52%	68.25%

percentages for the skull and skin are relatively consistent across both groups. This suggests that the processing techniques were equally effective in reducing point cloud sizes regardless of the size of the analyzed CT scan.

We compared the processed point clouds to the originals as well as the original mesh models to test for deviations. All skull and skin point cloud models showed perfect alignment and no outliers or deviations were present. When analyzing the point cloud models more closely we found that the average maximum error for the skull model was 0,730368 and 0,805882 for the skin model, being well within the acceptable range for DFR. In addition when comparing the point clouds with the original mesh segmentations we found the average distance between the skin mesh and point cloud was 0,00331060 and between the skull mesh and point cloud was 0,00260404. The largest distances were found in the areas of the back of the head and in the largest and most complex CT scans. This can be attributed to factors such as segmentation accuracy, simplification process limitations, and alignment considerations. Specifically, as the point clouds underwent an additional cleaning process when compared to the original STL files. In addition, a mitigating factor is the fact that the back of the head is not used for facial reconstruction, and is cut out for easier processing.

In addition, upon aligning and comparing the reduced point clouds and comparing them to the originals, we observed interesting patterns in the distance measurements across different facial regions between the bone and skin. The nasal area exhibited the largest distances, indicating potential differences in the shape and alignment of the nose between the point clouds. This finding suggests that the nose may have distinct variations and deviations in different individuals or scanning sessions, which could impact subsequent DFR or analyses.

Conversely, we found that the forehead area, superorbital area, and certain parts of the cheeks exhibited the smallest distances. These regions displayed closer alignment and similarity between the point clouds, indicating consistent facial features in these areas. This observation suggests that these regions may have less variability and are more reliable for precise DFR and analysis.

Overall, our results highlight the effectiveness of the point cloud reduction techniques employed, as well as the importance of accurately aligning and comparing point clouds for reliable DFR. These findings contribute to the advancement of DFR methodologies and provide valuable insights into the variations and consistencies within point cloud data.

6 Discussion

The results of our study demonstrate a significant reduction in the size of the point cloud models while maintaining clarity and preserving a high level of detail. The smaller size of the point clouds enables faster processing and analysis, as computational operations can be performed more efficiently. This can lead to improved turnaround times and increased productivity in the field of DFR.

It is observed that larger and more complex skull and facial skin models tend to respond better to the processing, resulting in a larger reduction of points of the point cloud, while still preserving important details. This could be because larger point clouds inherently contain more data points, capturing a higher level of detail and intricacies of the scanned object. This increased level of detail allows for a more accurate representation of the bone and skin structures, resulting in improved results. Additionally, larger point clouds provide a denser

Table 2: Acceptance criteria and alignment check

Scan ID	Avg. Dist. Skin	Avg. Dist. Skull	Error Skin	Error Skull
1	0.00281830	0.00256553	0.857123	0.776819
2	0.01277510	0.00469573	0.836600	0.754045
3	0.00394878	0.00265517	0.825804	0.753992
4	0.00106718	0.00321285	0.843168	0.753699
5	0.00332792	0.00288330	0.823054	0.721549
6	0.00234217	0.00609075	0.861356	0.720610
7	0.00200455	0.00609103	0.887325	0.720610
8	0.00358644	0.00336779	0.843581	0.820974
9	0.01041560	0.00344334	0.871147	0.820132
10	0.00090295	0.00016398	0.741171	0.668090
11	0.00045204	0.00013618	0.723477	0.667988
12	0.00155575	0.00022674	0.727078	0.670085
13	0.00319508	0.00314697	0.808749	0.770929
14	0.00054517	0.00025358	0.717866	0.668009
15	0.00072191	0.00012763	0.720730	0.667982

sampling of the surface, which leads to a more precise reconstruction. The additional points enable the capture of finer features, such as subtle variations in curvature or small surface irregularities.

Furthermore, larger point clouds provide a more robust foundation for subsequent processing steps, such as alignment and comparison. The increased number of points enhances the stability and reliability of these operations, allowing for more accurate registration and analysis of the models.

However, it is noted that there are certain areas that could be improved, the data suggest that problems with segmentation mainly occurred when segmenting the left side of the faces due to distortion caused by the subjects being pressed against the scanner. Addressing these issues and refining the segmentation process could result in more precise and accurate models.

Additionally, the data reveals the presence of residual soft tissue in some skin scans, which could not be segmented and was subsequently filtered out during the processing in MeshLab. This implies that there might be a need for more advanced segmentation techniques or additional manual intervention to overcome challenges related to soft tissue segmentation.

Furthermore, some smaller bone fragments located inside the skull also needed to be filtered out in a similar manner. This highlights the importance of carefully assessing the specific requirements of the DFR application and tailoring the processing steps accordingly to remove any unwanted or irrelevant structures while maintaining the integrity of the main bone and skin models.

In addition, there is still room for further improvement in the processing of the point cloud models. Advanced point cloud refinement techniques, such as noise reduction, outlier removal, and surface reconstruction, can be implemented to enhance the quality and accuracy of the data. To further improve processing we plan on experimenting with more prominent tools, such as MATLAB.

Another avenue for improvement lies in feature-based compression methods. By selectively preserving important anatomical features and prioritizing the representation of critical facial landmarks and regions, we can maintain the necessary precision for DFR while reducing the overall data size. This approach allows us to strike a balance between size and detail, optimizing the efficiency of storage and processing resources.

Finally, the construction of a dedicated head CT dataset for DFR would be an important tool. Having a dedicated dataset for DFR would ensure that the data is standardized and optimized for accurate and reliable reconstruction outcomes. Such a dataset could encompass a diverse range of head CT scans with varying anatomical features, STT, and pathologies, providing a comprehensive representation of the human population. Additionally, it would enable researchers and practitioners to focus their efforts on refining algorithms and techniques specifically tailored for DFR, leading to advancements in accuracy, speed, and efficiency. Moreover, a well-curated dataset would facilitate benchmarking and comparison of different reconstruction approaches, promoting collaboration and knowledge sharing within the research community. Ultimately, the availability of a dedicated head CT dataset would greatly contribute to the development and improvement of DFR methods, enabling enhanced clinical applications, forensic investigations, and facial prosthetics.

Overall, while the presented data demonstrates the successful reduction of point cloud size and the preservation of important details in skull and facial skin models, there are areas that warrant further investigation and refinement. Improving CT image segmentation,

addressing challenges related to distorted scans and soft tissue segmentation, and adapting the processing steps to filter out unwanted structures will contribute to the continued enhancement of the accuracy and precision of the point cloud models, ultimately advancing the field of DFR.

7 Conclusion

In conclusion, our paper has covered various aspects of DFR, CT image processing, and point cloud comparison. We explored different open-source tools and techniques used in these processes, including 3D Slicer, MeshLab, CloudCompare, and their respective functionalities. We also discussed the importance of data formats, such as DICOM and STL.

Furthermore, we examined the outcomes of the image processing steps performed in 3D Slicer, MeshLab, and the reduction in point cloud size achieved through simplification and cropping. The reduction in point cloud size was substantial, with the bone point clouds being reduced by 91.13% on average and the skin point clouds being reduced by 80.35%. We also analyzed the alignment and comparison of the processed point clouds with the original point clouds and found perfect alignment with no outliers or deviations. Finally, we were looking at the relationship between the skull and skin point clouds and found that the largest distances were observed in the nasal area, while the smallest distances were recorded in the forehead, superorbital, and cheek regions.

Moreover, we discussed potential areas for improvement, including employing advanced segmentation and point cloud refinement techniques, feature-based compression methods, and adaptive level of detail approaches to enhance the precision of point cloud models while keeping them at a small size. These strategies can contribute to more accurate DFR, faster processing, and improved efficiency in facial analysis.

Overall, the presented results highlight the complexity and potential of DFR, CT image processing, and point cloud comparison. We demonstrated the importance of utilizing appropriate tools, considering data formats, and implementing optimization techniques to achieve precise and efficient results. Continued advancements in these areas will pave the way for significant applications in fields such as forensic reconstruction, medical imaging and beyond.

References

Miranda, G. E., Wilkinson, C., Roughley, M., Beaini, T. L., & Melani, R. F. H. (2018). Assessment of accuracy and recognition of three-dimensional computerized forensic craniofacial reconstruction. *PLoS One*, 13(5), e0196770.

Ulinuha, M. A., Yuniarno, E. M., Hariadi, M., & Purnama, I. K. E. (2019, March). Extraction of skull and face surfaces from CT images. In 2019 *International Conference of Artificial Intelligence and Information Technology (ICAIIT)* (pp. 37-40). IEEE.

Simmons-Ehrhardt, T., Falsetti, C., Falsetti, A. B., & Ehrhardt, C. J. (2018). Open-source tools for dense facial tissue depth mapping of computed tomography models. *Human biology*, 90(1), 63-76.

da Costa Moraes, C. A., Dias, P. E. M., & Melani, R. F. H. (2014). Demonstration of protocol for computer-aided forensic facial reconstruction with free software and photogrammetry. *Journal of Research in Dentistry*, 2(1).

Hargreaves, M., Ting, D., Bajan, S., Bhavnagri, K., Bassed, R., & Chang, X. (2021, November). A Generative Deep Learning Approach for Forensic Facial Reconstruction. In 2021 *Digital Image Computing: Techniques and Applications (DICTA)* (pp. 1-7). IEEE.

Duan, F., Huang, D., Tian, Y., Lu, K., Wu, Z., & Zhou, M. (2015). 3d face reconstruction from skull by regression modeling in shape parameter spaces. *Neurocomputing*, 151, 674-682.

Ma, T. C., Nguyen, D. T., Dinh, Q. H., & Bui, T. D. (2011, October). 3D facial reconstruction system from skull for Vietnamese. In 2011 *Third International Conference on Knowledge and Systems Engineering* (pp. 120-127). IEEE.

Shui, W., Zhou, M., Deng, Q., Wu, Z., & Duan, F. (2010, November). 3D craniofacial reconstruction using reference skull-face database. In 2010 *25th International Conference of Image and Vision Computing New Zealand* (pp. 1-7). IEEE.

3D Slicer image computing platform (2023). Retrieved from https://slicer.org/

Cignoni, P., Callieri, M., Corsini, M., Dellepiane, M., Ganovelli, F., & Ranzuglia, G. (2008, July). Meshlab: an open-source mesh processing tool. In *Eurographics Italian chapter conference* (Vol. 2008, pp. 129-136).

CloudCompare - Open Source project (2023). Retrieved from https://www.danielgm.net/cc/

CQ500 - V7 Open Datasets (2023). Retrieved from https://www.v7labs.com/open-datasets/cq500